Supporting Information

Instruments

The as-prepared nanostructures on the substrate were sent to characterizations on a CAMSCAN APOLLO 300 field-emission scanning electron microscopy (FE-SEM) at 15KV. The crystal structure of the products was studied using a Bruker D8 X-ray diffractometer with Cu Kα irradiation at λ = 1.5406 Å. For high-resolution TEM measurements, one drop of the alcohol dispersed suspension of sample was placed on a carbon-coated copper grid and allowed to dry in air. The grid was then observed on a Tecnai GF2 operated at an accelerating voltage of 400 kV. Selected area electron diffraction (SAED) patterns were also obtained. The absorbance spectrum of AMA Ag samples were measured using a PerkinElmer Lambda35 fiber-optic UV-vis NIR spectrophotometer.

SEM Measurements

Figure S1. FE-SEM image of silicon pillar arrays with 2μM × 2μM between each silicon pillar gap, the arrangement of a square, and 20μM etching depth of silicon column.

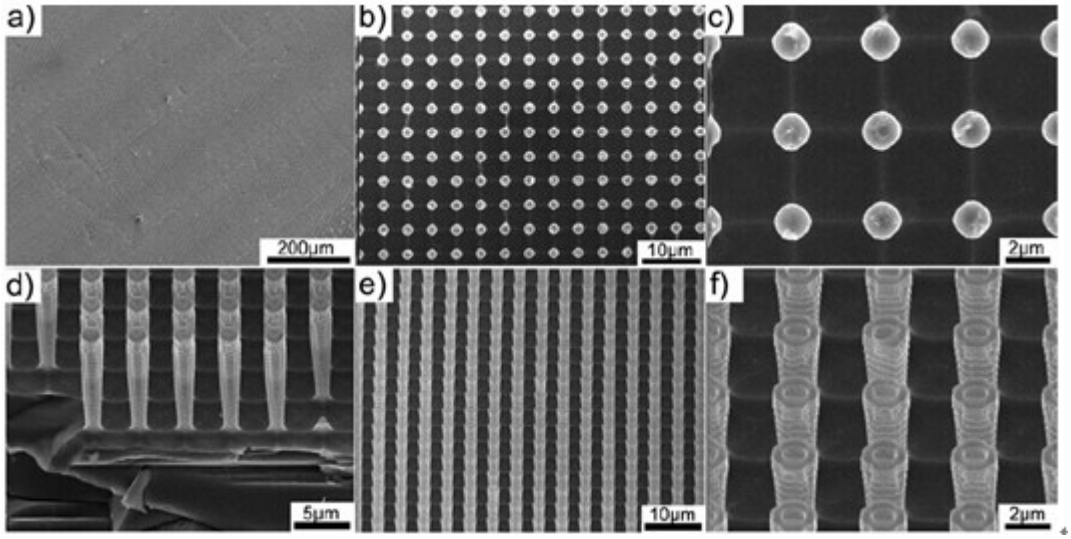

Figure S2. FE-SEM image of silicon pillar arrays with 2μM × 2μM between each silicon pillar gap, the arrangement of regular hexagon, and 20μM etching depth of silicon column.

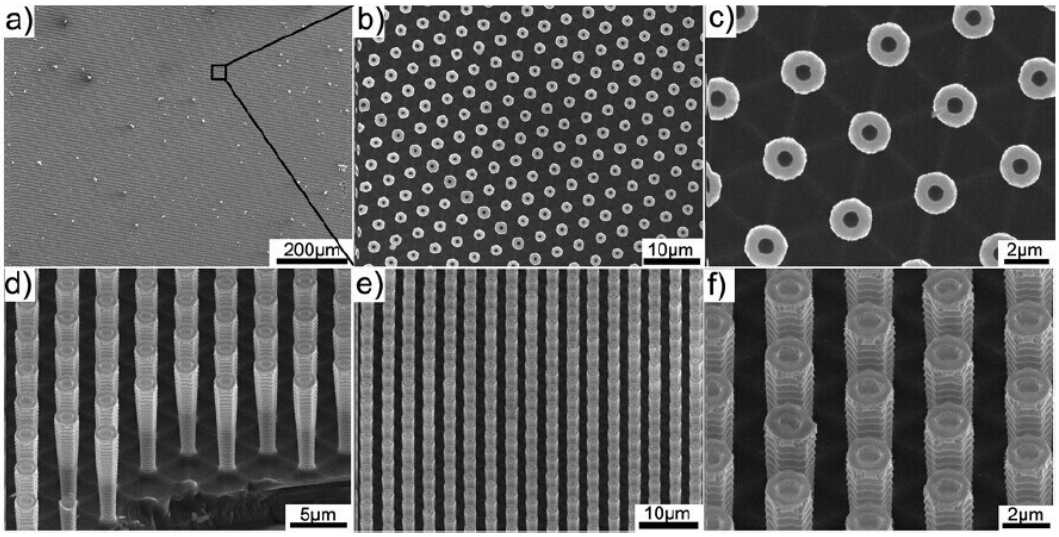

Figure S3. FE-SEM image of silicon pillar arrays with 2μM × 2μM between each silicon pillar gap, the arrangement of a square, and 10μM etching depth of silicon column.

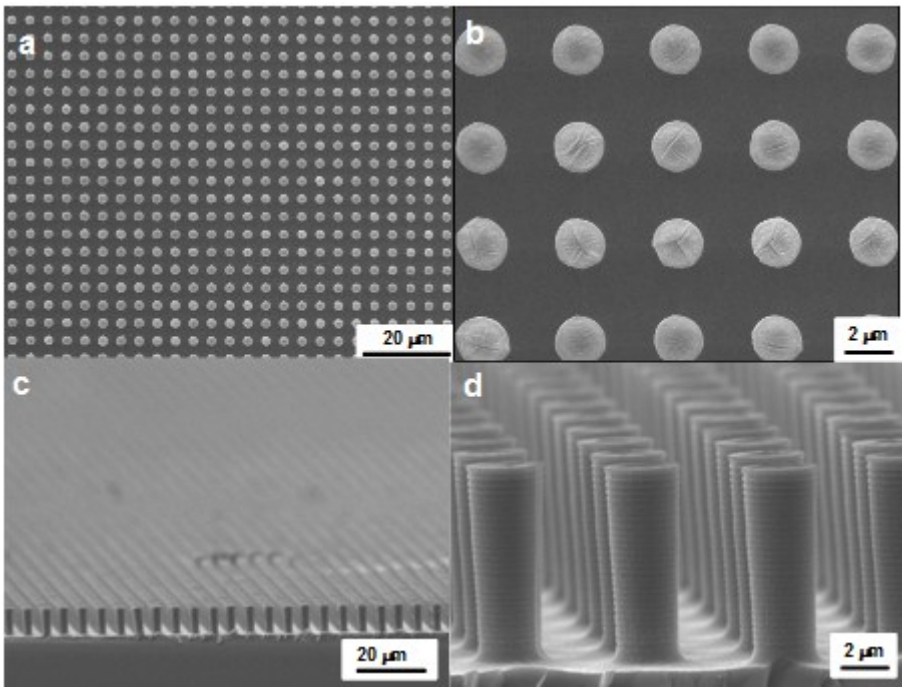

Figure S4. FE-SEM image of silicon pillar arrays with 4μM × 4μM between each silicon pillar gap, the arrangement of a square, and 10μM etching depth of silicon column.

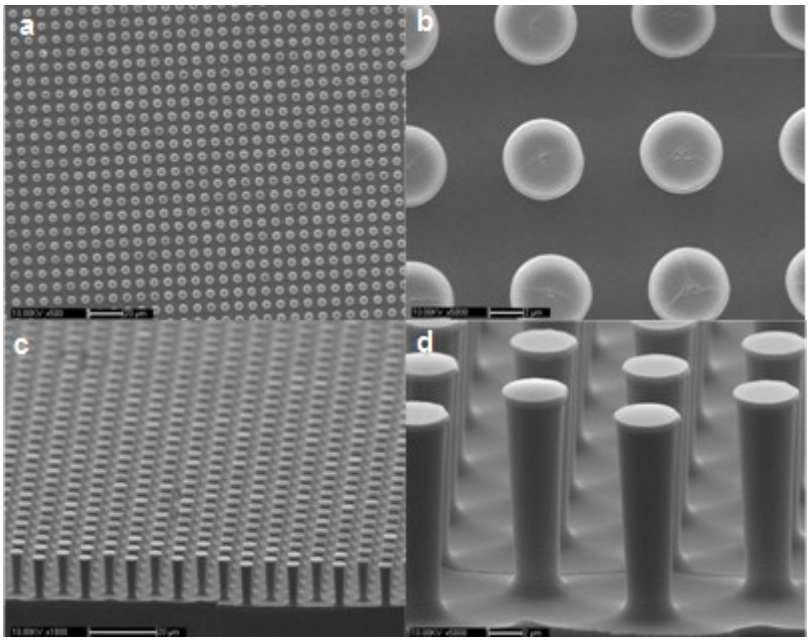

Figure S5. FE-SEM image of AMA substrates with silicon pillar arrays template (4μM × 4μM between each silicon pillar gap, the arrangement of a square, and 10μM etching depth of silicon column)

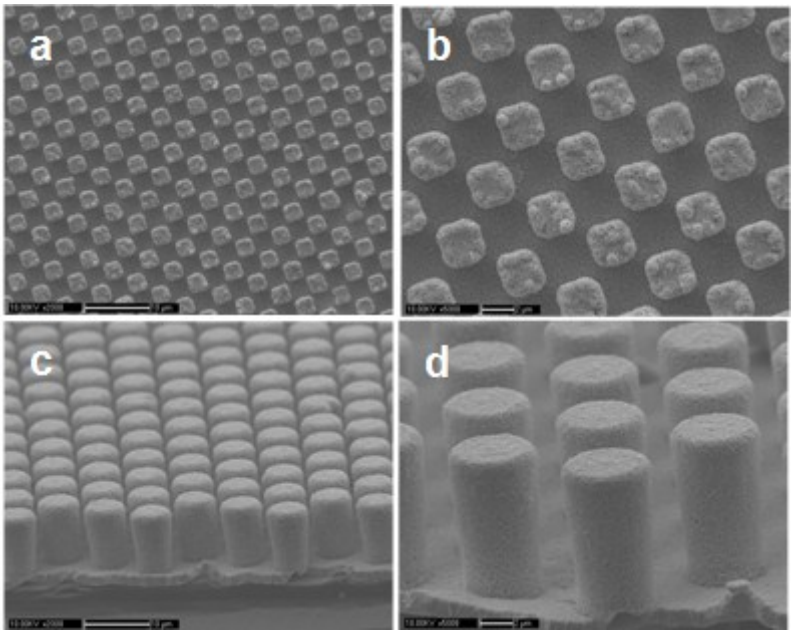

Figure S6. FE-SEM image of AMA substrates with silicon pillar arrays template (4μM × 4μM between each silicon pillar gap, the arrangement of regular hexagon , and 10μM etching depth of silicon column)

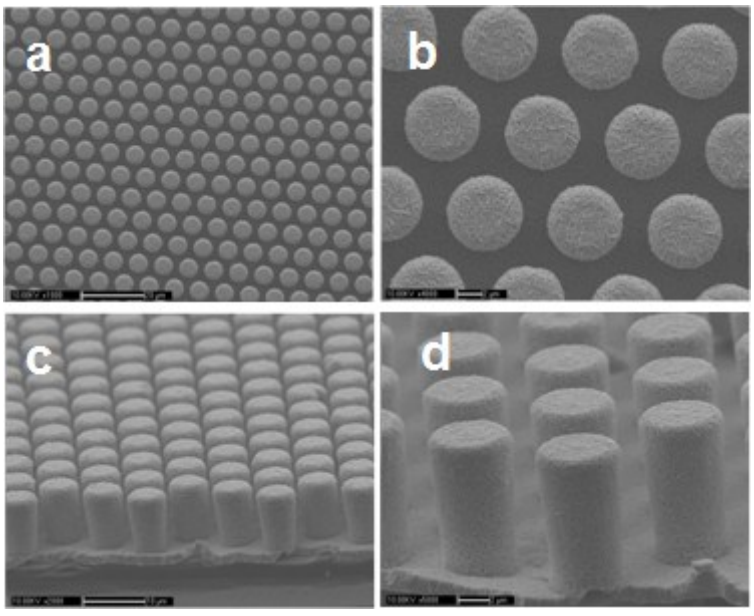

Figure S7. FE-SEM image of AMA substrates with silicon pillar arrays template (2μM × 2μM between each silicon pillar gap, the arrangement of a square, and 20μM etching depth of silicon column, and the electrochemical deposition procedure time was 2h, the current density was set for 200 μA).

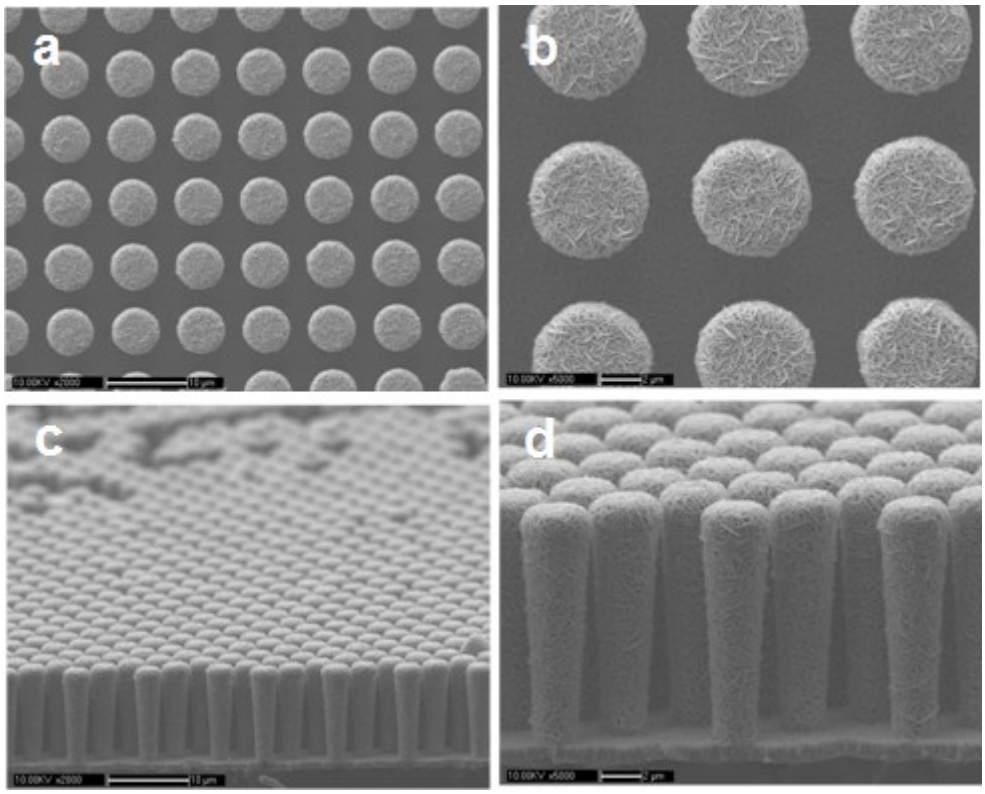

Figure S8. FE-SEM image of AMA substrates with silicon pillar arrays template (2μM × 2μM between each silicon pillar gap, the arrangement of a square, and 20μM etching depth of silicon column, and the electrochemical deposition procedure time was 3h, the current density was set for 200 μA).

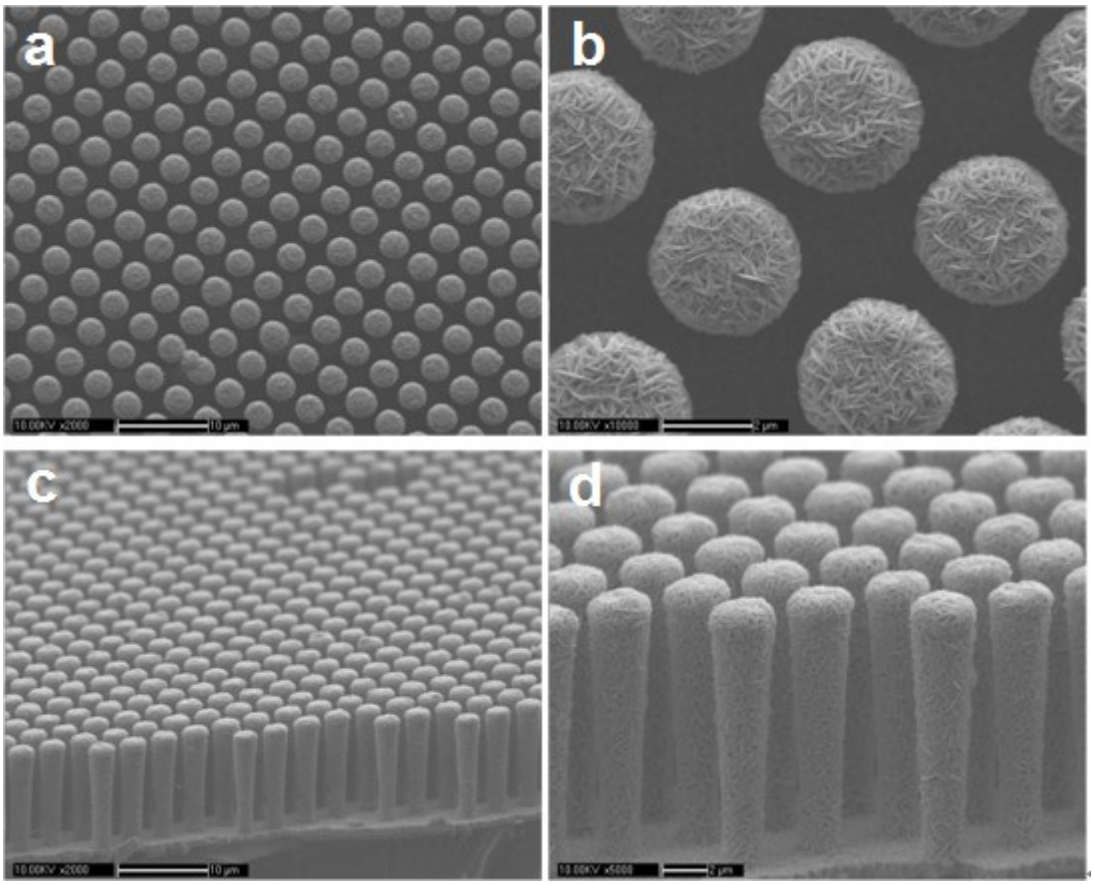

Figure S9. FE-SEM image of AMA substrates with silicon pillar arrays template (2μM × 2μM between each silicon pillar gap, the arrangement of a square, and 20μM etching depth of silicon column, and the electrochemical deposition procedure time was 4h, the current density was set for 200 μA).

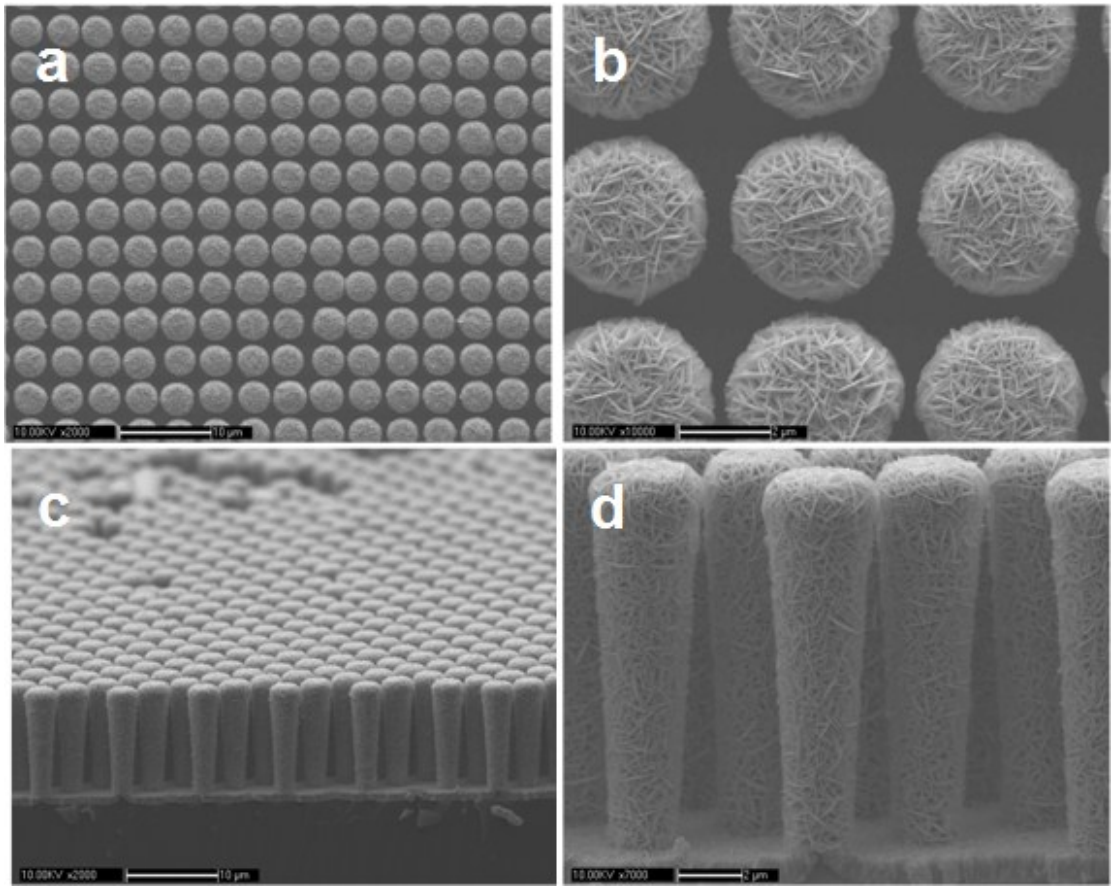

Figure S10. FE-SEM image of AMA substrates with silicon pillar arrays template (2μM × 2μM between each silicon pillar gap, the arrangement of a square, and 20μM etching depth of silicon column, and the electrochemical deposition procedure time was 5h, the current density was set for 200 μA).

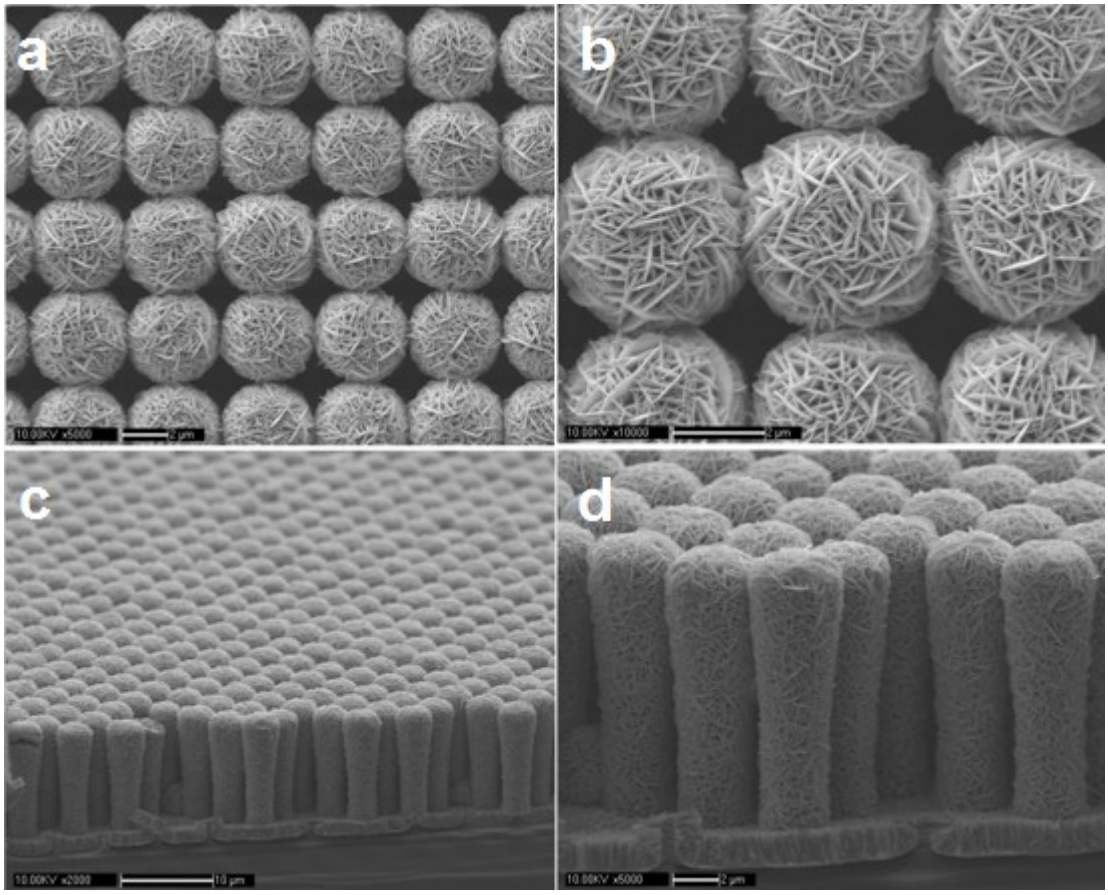

Figure S11. FE-SEM image of AMA substrates with silicon pillar arrays template (2μM × 2μM between each silicon pillar gap, the arrangement of a square, and 20μM etching depth of silicon column, and the electrochemical deposition procedure time was 6h, the current density was set for 200 μA).

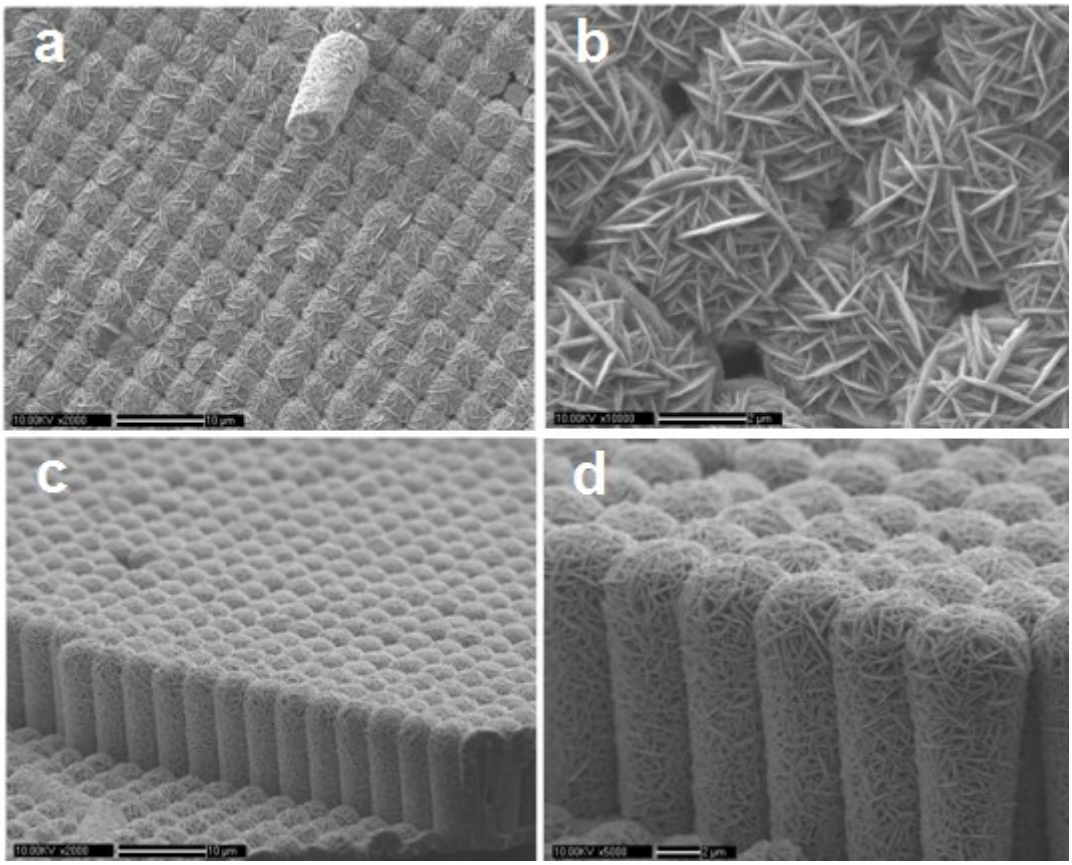

Figure S12. FE-SEM image of AMA substrates with silicon pillar arrays template (2μM × 2μM between each silicon pillar gap, the arrangement of a square, and 20μM etching depth of silicon column, and the electrochemical deposition procedure time was 7h, the current density was set for 200 μA).

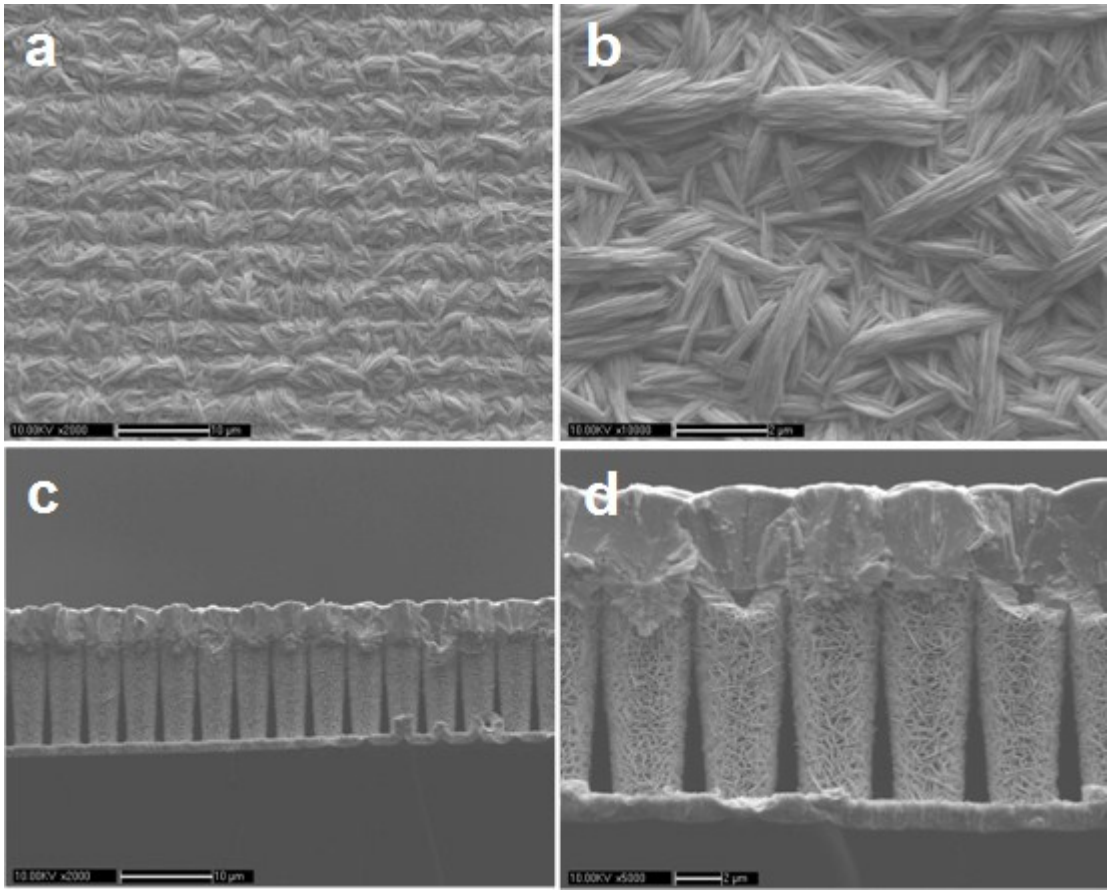

Figure S13. XRD patterns of AMA substrates.

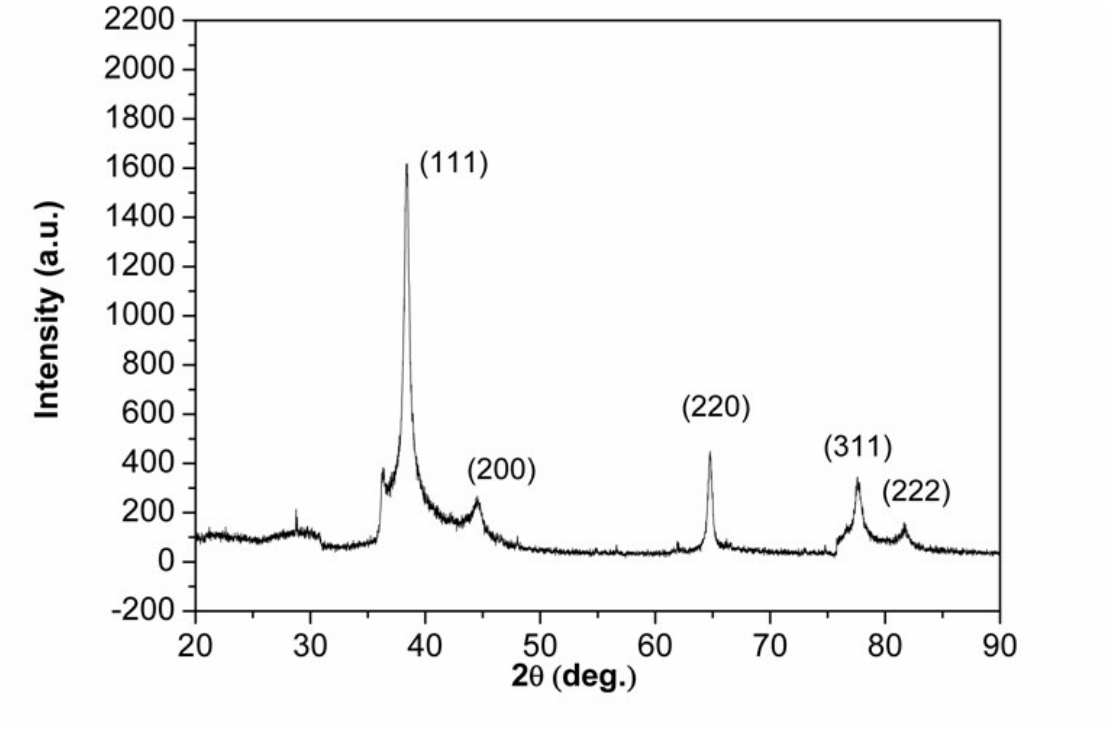

Figure S14. UV-vis analysis of AMA substrate with 6h Ag deposition time.

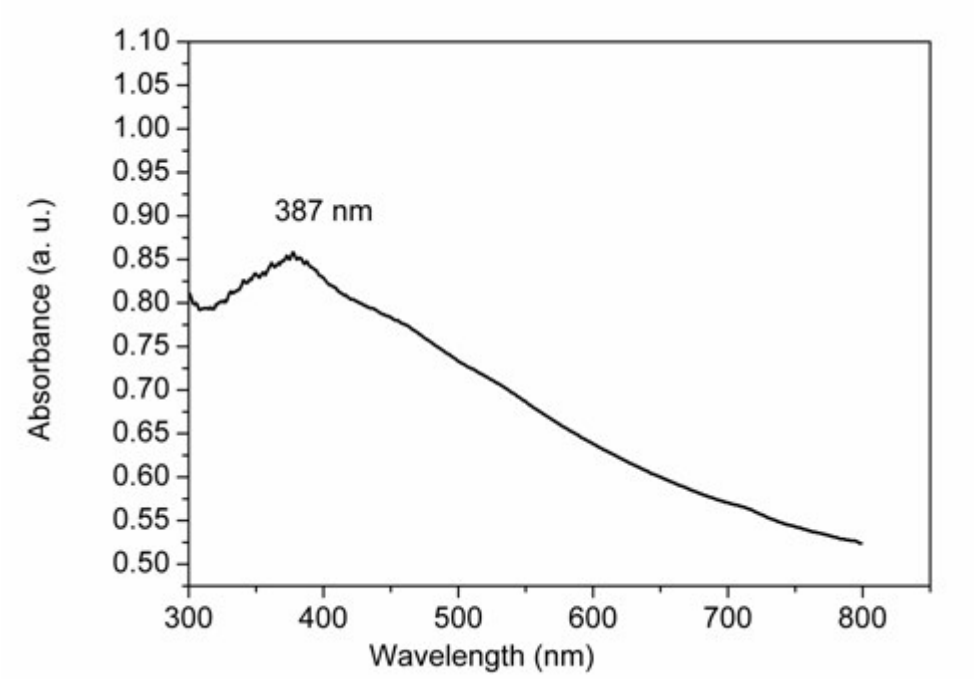

Figure S15 The water contact angle (CA) of AMA slim prepared from

temple ③ in Figure 3, the water contact angle is 153°.

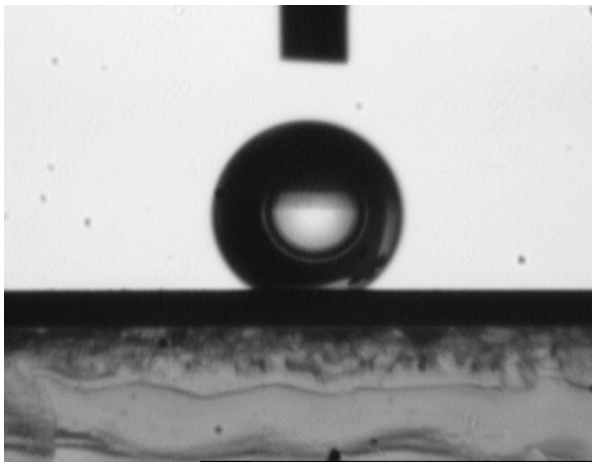

Figure S16 The water contact angle (CA) of AMA slim prepared from temple ④ in Figure 3，the water contact angle is 152°.

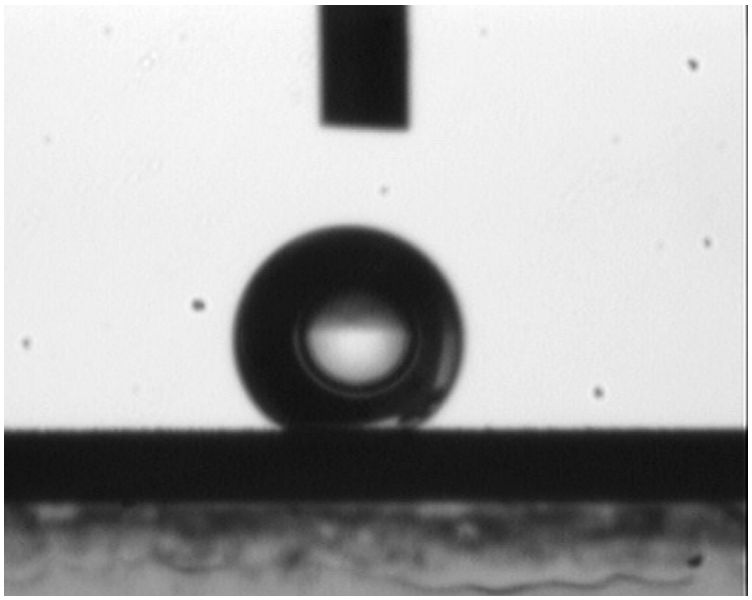

Estimation of enhancement factor

We used the peak at 611 cm^{-1} (for R6G) to estimate the enhancement factor (EF). The SERS EF is a quantitative measure of the Raman signal amplification of an analyte. We calculated this value using the reported protocol. [1] The EF can be calculated by:

$$EF = \frac{I_{SERS} N_{Ref}}{I_{Ref} N_{SERS}}$$

Where N_{SERS} and N_{Ref} are the number of molecules probed on the nanoflower and on the reference sample, respectively. I_{SERS} and I_{Ref} correspond to SERS signal and the un-enhanced normal signals intensities, respectively. Herein, a certain volume (V_{SERS}) and concentration (C_{SERS}) R6G aqueous solution was dispersed to an area of Raman concentration for non-SERS Raman spectra certain S_{SERS} at the AMA substrate. For non-SERS Raman spectra, a certain volume (V_{Ref}) and concentration (C_{Ref}) R6G aqueous solution was dispersed to an area of S_{Ref} at a clean Si substrate. Both the substrates were dried in the air. Considering the area of laser spot is the same, the foregoing equation thus becomes:

$$EF = \frac{I_{SERS}}{I_{Ref}} \bullet \frac{C_{Ref} V_{Ref}}{C_{SERS} V_{SERS}} \bullet \frac{S_{SERS}}{S_{Ref}}$$

In our experiment, 1 μL of 1×10^{-11} M R6G solution was dispersed to an area of 10 mm^2 for the AMA substrate shown in Figure S18 and 1 μL of

1×10^{-3} M R6G ethanol solution was dispersed to an area of π mm^2 for the silicon wafer. For the band at 611 cm^{-1}, I_{SERS} /I_{Ref} was 1369/180=7.61. Therefore average enhancement factor for the band at 611 cm^{-1} is calculated to be 2.42×10^9 . With the same method, the Efs for the SERS substrates shown in Figure S17, S18 were estimated to be 2.42×10^9.

Figure S17. The SERS spectra of R6G collected on the 3D AMA substrates with different concentration of R6G 1×10^{-13}M to 1×10^{-15}M.

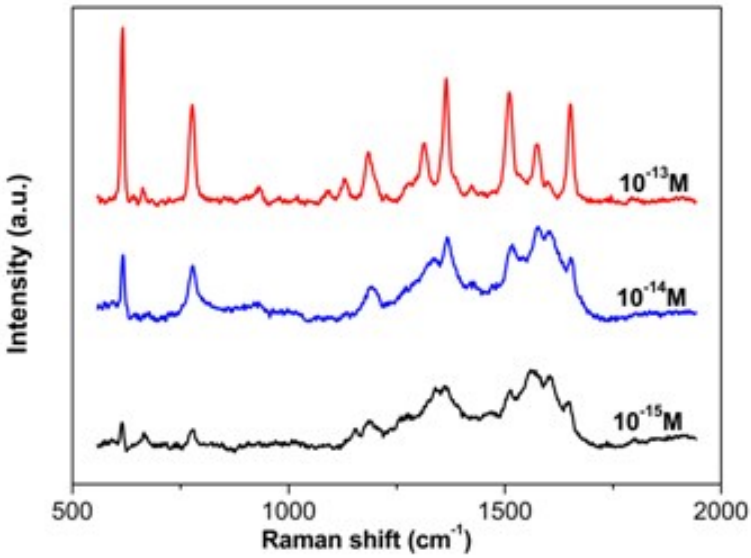

Figure S18. The SERS spectra of R6G collected on the 3D AMA substrates

with concentration of R6G 1×10^{-11}M and the Raman spectra of R6G collected on the Si wafer with concentration of 1×10^{-3}M for comparison.

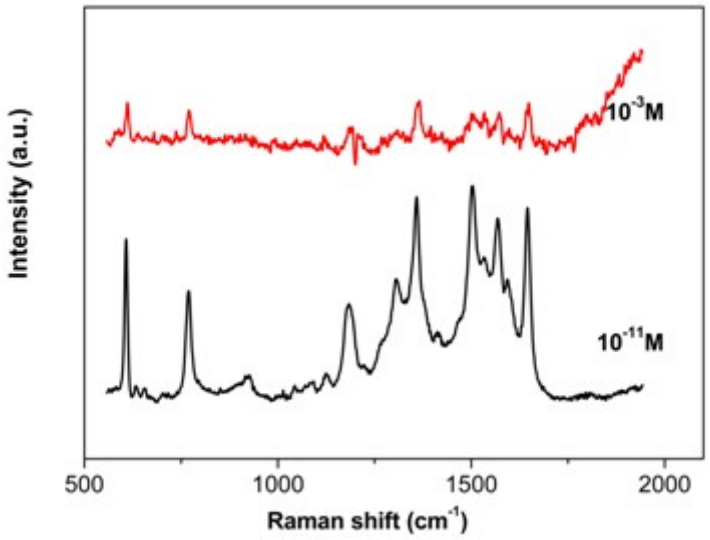

Figure S19. Vibrational mode of PA.

At the same level of theory, the frequencies and Raman intensities were calculated at the optimized geometry. The band at 824 cm^{-1} due to the O-H out of plane molecule stretching vibration and 1085 cm^{-1} due to the totally symmetric C–H stretching mode was significantly enhanced. The Raman bands at 1312 cm^{-1}, allocated to NO_2 symmetric stretching vibration. And the Raman bands at 1531cm^{-1}, allocated to NO_2 asymmetric stretching vibration. The totally symmetric C–H stretching mode(1094cm^{-1}), shift to 1085cm^{-1}. This shift might depend on the direction of the local electrical field at the molecular adsorption site and the molecular orientation with respect to the nanostructure surface.

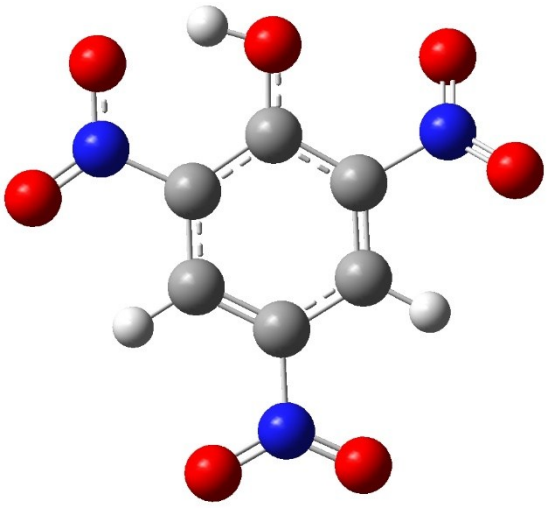

Table S1 Assignment of SERS and the vibrational description for PA[2]

Vibrational description	SERS assignment
ν(CC) [a]	1635
$\nu_{as}(NO_2)$	1531
$\nu_{s}(NO_2)$	1312
δ(CH) [b]	1272
δ(CH)	1085
δ(OH)-out of plane	824

[a] ν, stretching; [b] δ, bending.

Figure S20. the limit of detection of explosive PA

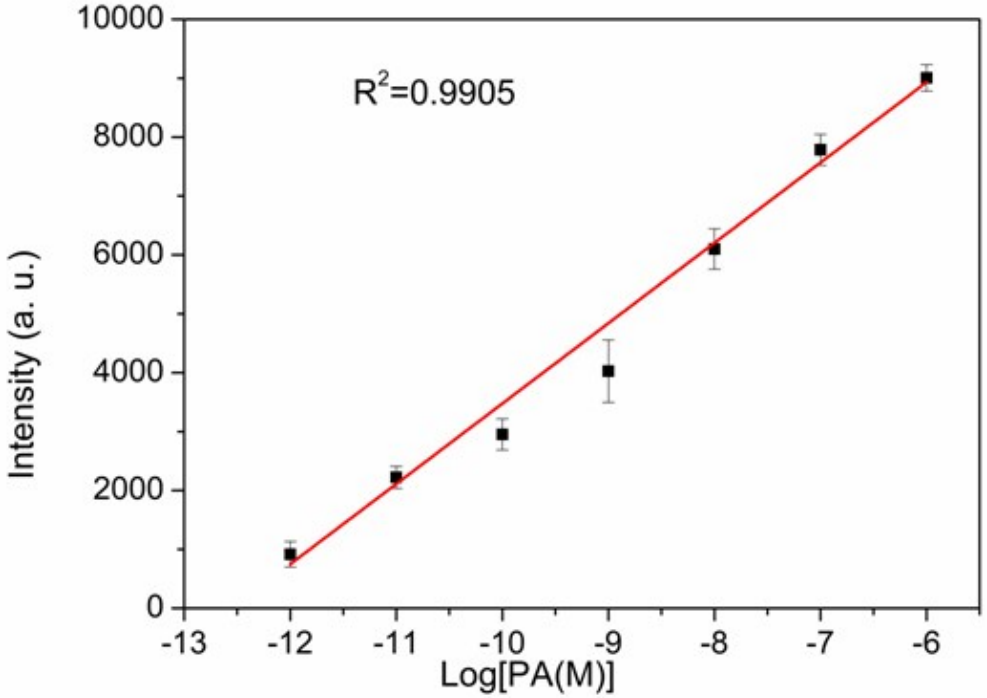

Figure S21. Vibrational mode of NTO

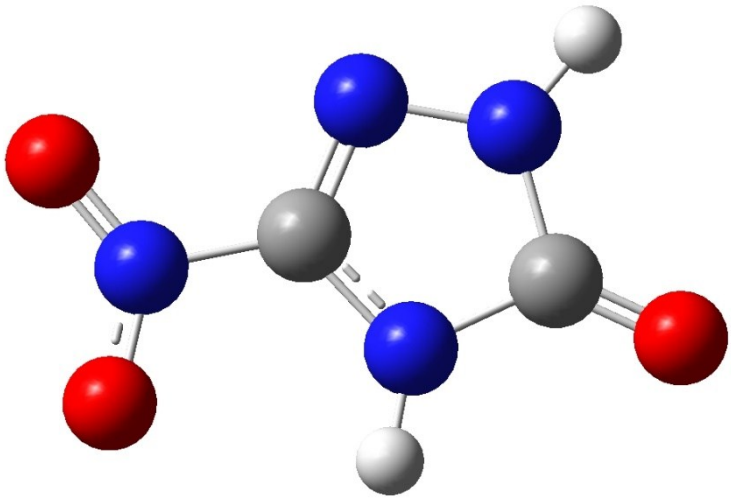

Table S2 Assignment of SERS and the vibrational description for NTO [3]

Vibrational description	SERS assignment
$\nu(NO_2)$ [a]	850
ν(C=C)ring	1062
δ(CH)ring [b]	1104
$\nu(NO_2)$	1308
$\nu(NO_2)$	1389

[a] ν, stretching; [b] δ, bending.

Figure S22. the limit of detection of explosive NTO

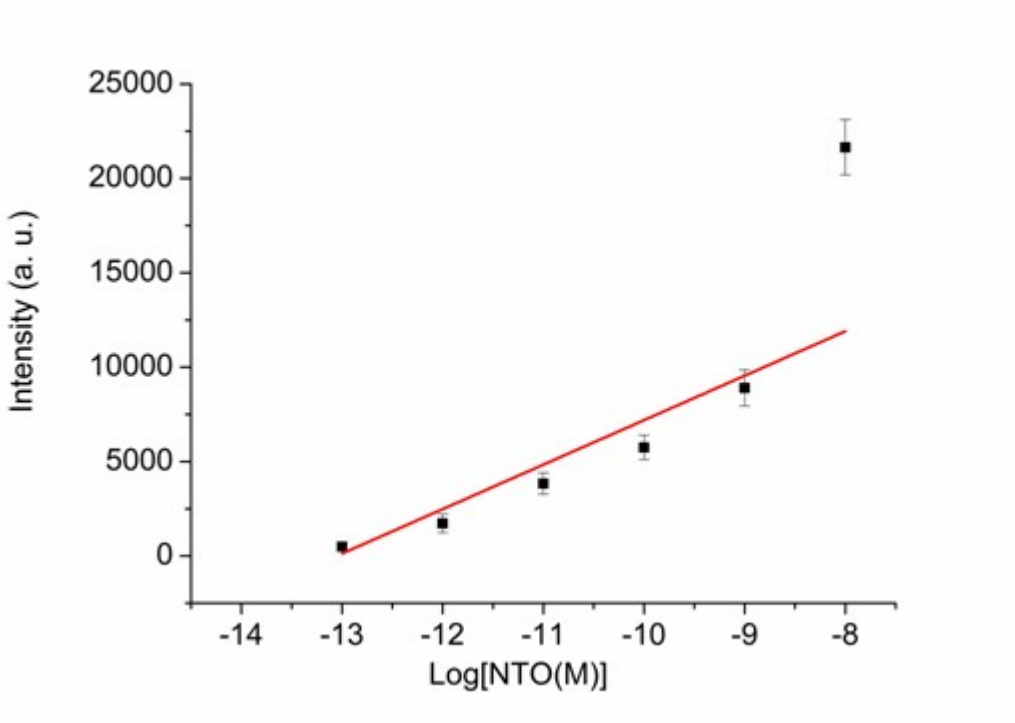

Figure S23. SERS spectra of PA (1×10^{-6} mol/L) molecules adsorbed on the 3D biomimetic superhydrophobic AMA substrates and Raman spectra of

solid PA;

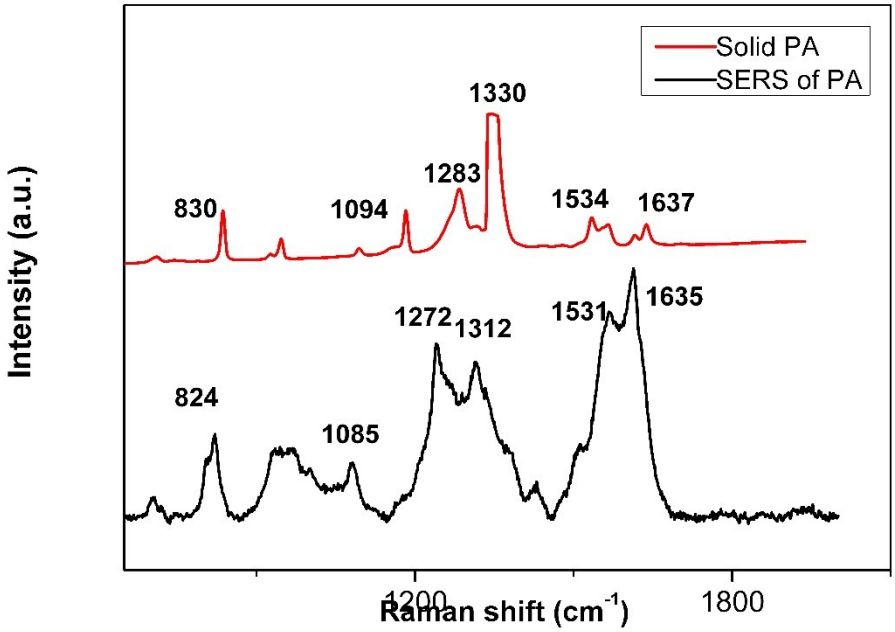

Tap water (10 mL) was chosen as the real samples to validate the feasibility of 3D biomimetic super-hydrophobic AMA SERS substrates in the analysis of explosives PA and NTO in real systems. A series of real system PA solution were prepared by diluting PA standard solution with tap water of varied volume ratios. Then, 3μL of different concentrations PA real system solution were dropped onto the surface of biomimetic super-hydrophobic AMA SERS substrates. The hydrophobic surfaces made the solution droplet to be a spherical shape on it and then it effectively inhibited solution droplet spreading around. The molecules in droplet would be concentrated and adsorbed on a small footprint area on nanoparticle arrays by rapid solvent evaporating. This process took only a few minutes to

condensate and absorb of detecting target molecules. At this point, we can see the characteristic Raman peak of the explosive PA at 824 cm^{-1} 1312 cm^{-1} and 1531 cm^{-1}. Then, we tested the NTO in the tap water in the same way, and the characteristic Raman peaks of the explosive NTO at 850, 1062, 1104, 1308, 1389 cm^{-1} could be clearly shown. It is indicated that the biomimetic AMA substrates have sensitive detection effect on actual sample detection experiments.

Figure S24 the experiments of PA in tap water

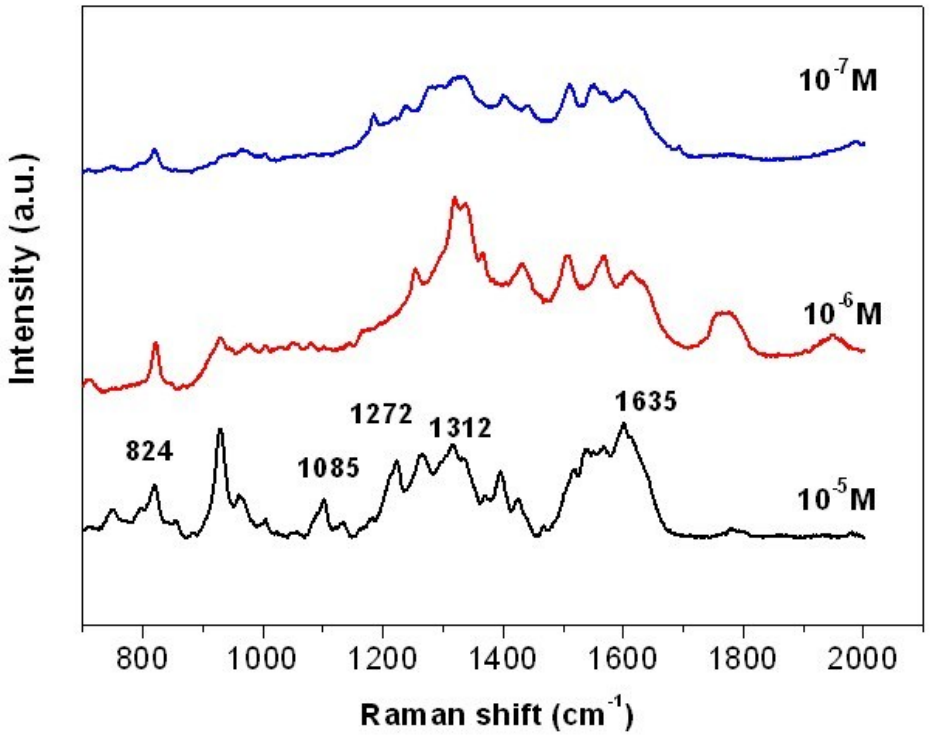

Figure S25 the experiments of NTO in tap water

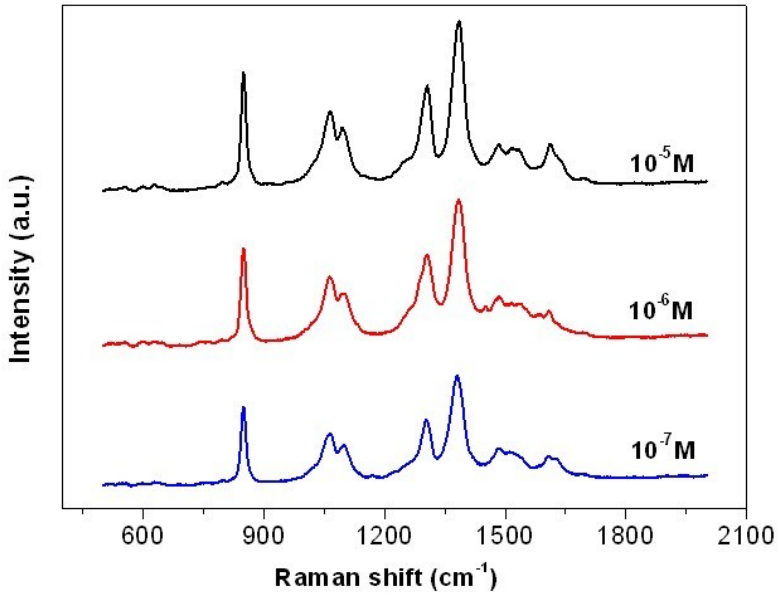

Figure S26 (a) the contact Angle of 100% ethanol as solution; (b) the contact Angle of 50% ethanol as solution; (c) the contact Angle of 20% ethanol as solution; (d) the contact Angle of 10% ethanol as solution; (e) the contact Angle of 100% water as solution.

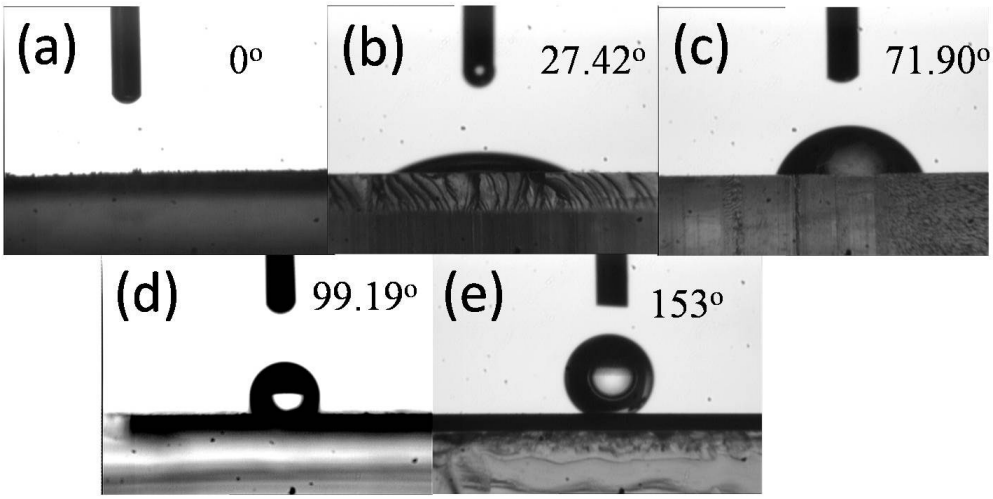

Figure S27 R6G solution(10^{-13}M) is dropped to the surface of SERS substrates, and the super-hydrophobic condensation strategy is used to detect it.

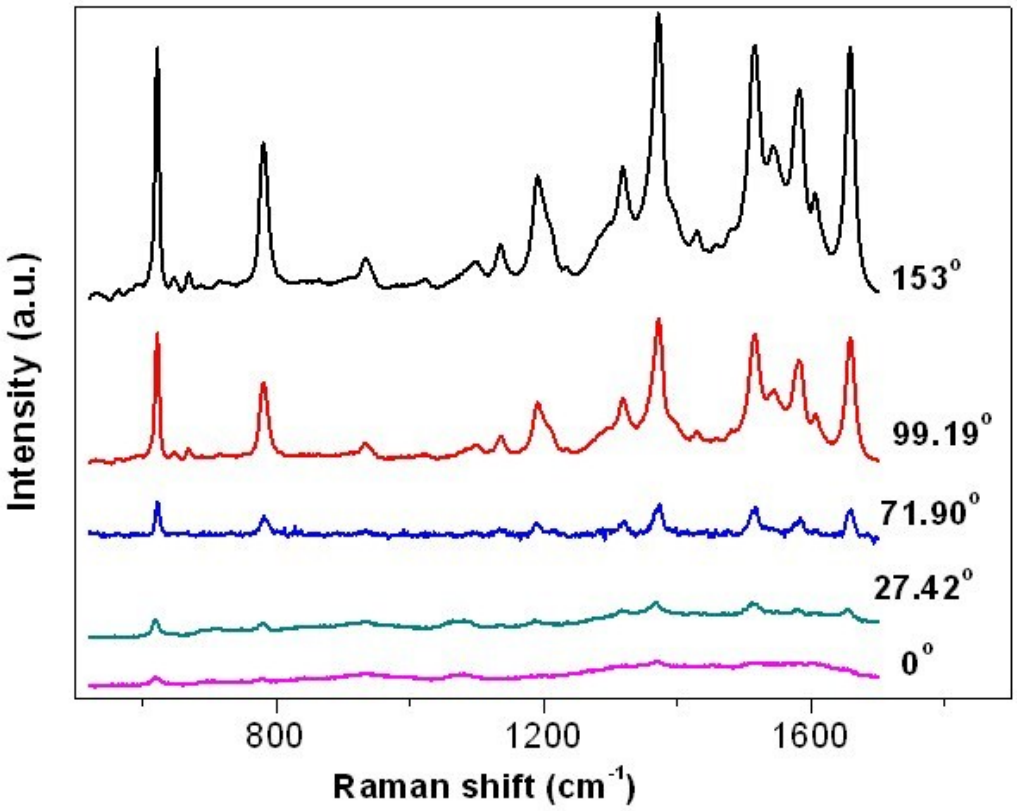

As the contact Angle increasing, the intensity of R6G Raman peaks enhance gradually.

Figure S28 explosive PA solution(10^{-11}M) is dropped to the surface of SERS substrates, and the super-hydrophobic condensation strategy is used to detect it.

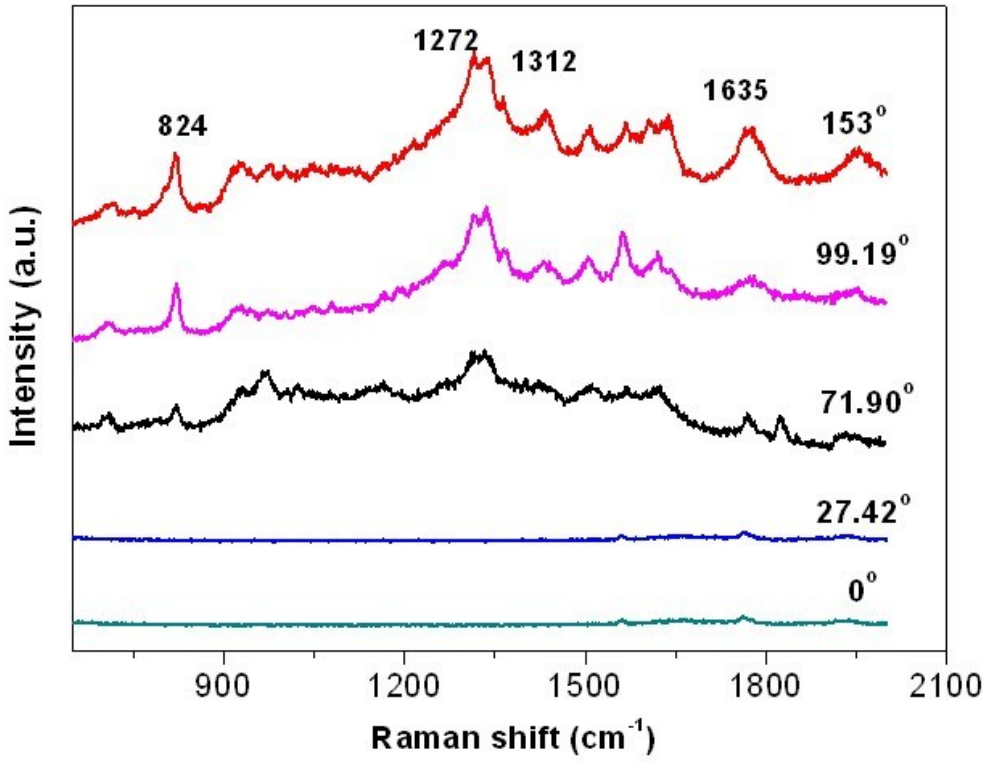

When the concentration of PA was 10^{-11}M, the Raman characteristic peaks of PA could be detected at the water contact Angle of 111.8° and 153°. In contrast, the contact Angle was 0°, 27.42°, 71.9°, the Raman characteristic peaks of the explosive PA could not be detected.

Figure S29 explosive PA solution(10^{-8}M) is dropped to the surface of SERS substrates, and the super-hydrophobic condensation strategy is used to detect it.

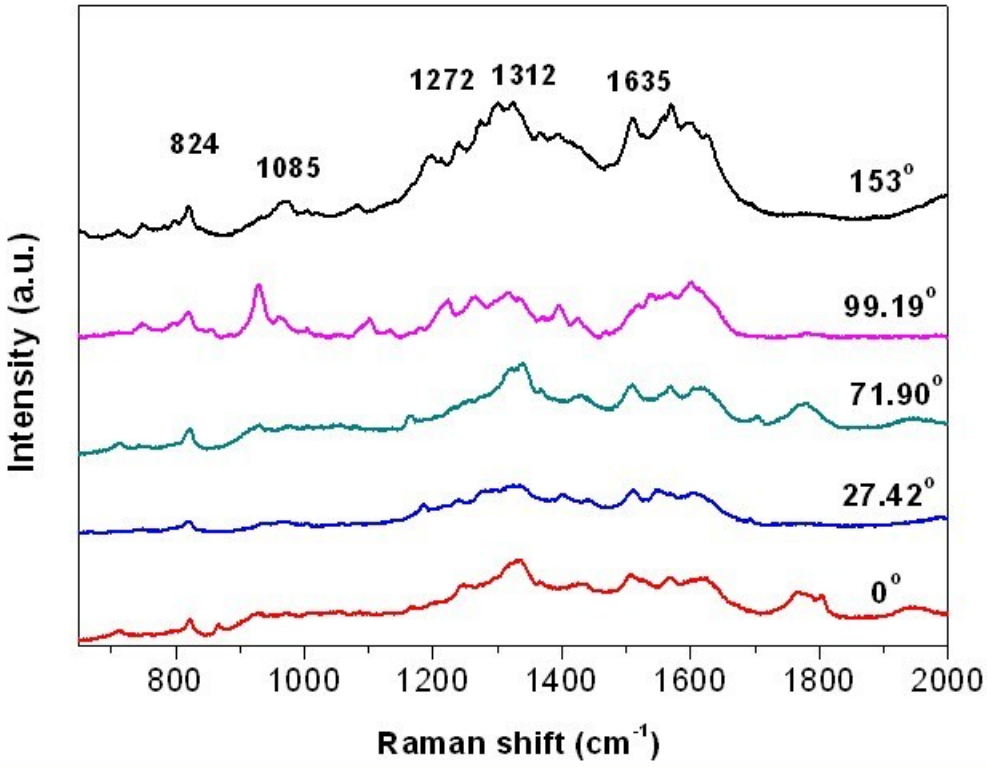

Figure S30 explosive NTO solution(10^{-11}M) is dropped to the surface of SERS substrates, and the super-hydrophobic condensation strategy is used to detect it.

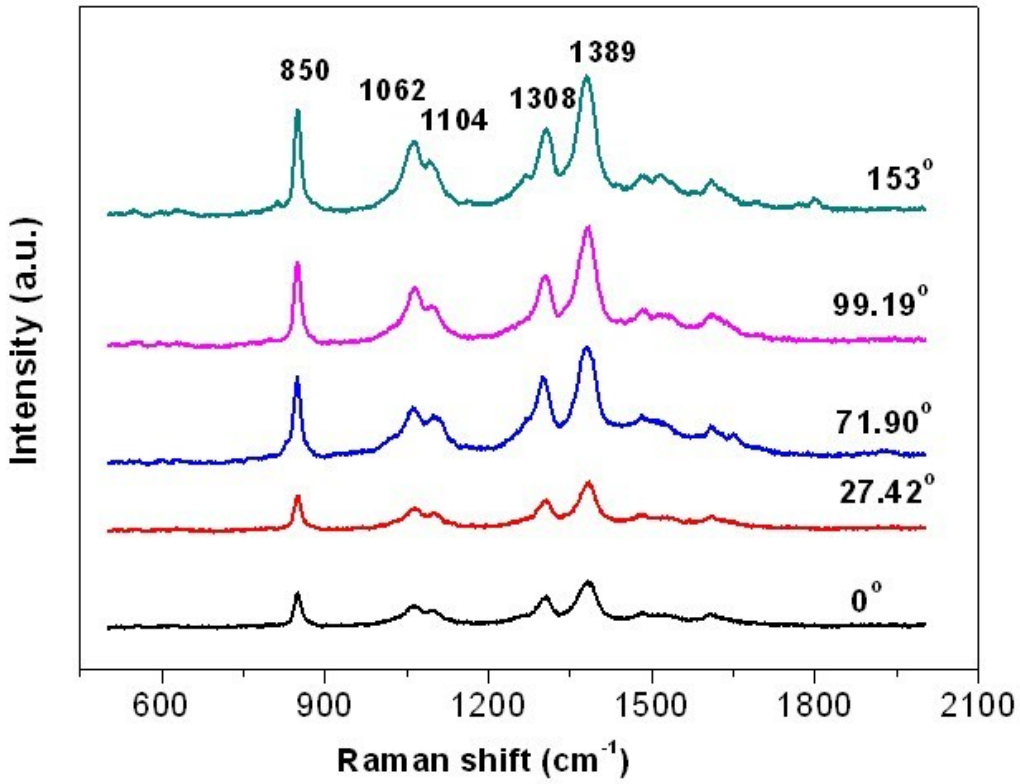

Figure S31 explosive NTO solution(10^{-8} M) is dropped to the surface of SERS substrates, and the super-hydrophobic condensation strategy is used to detect it.

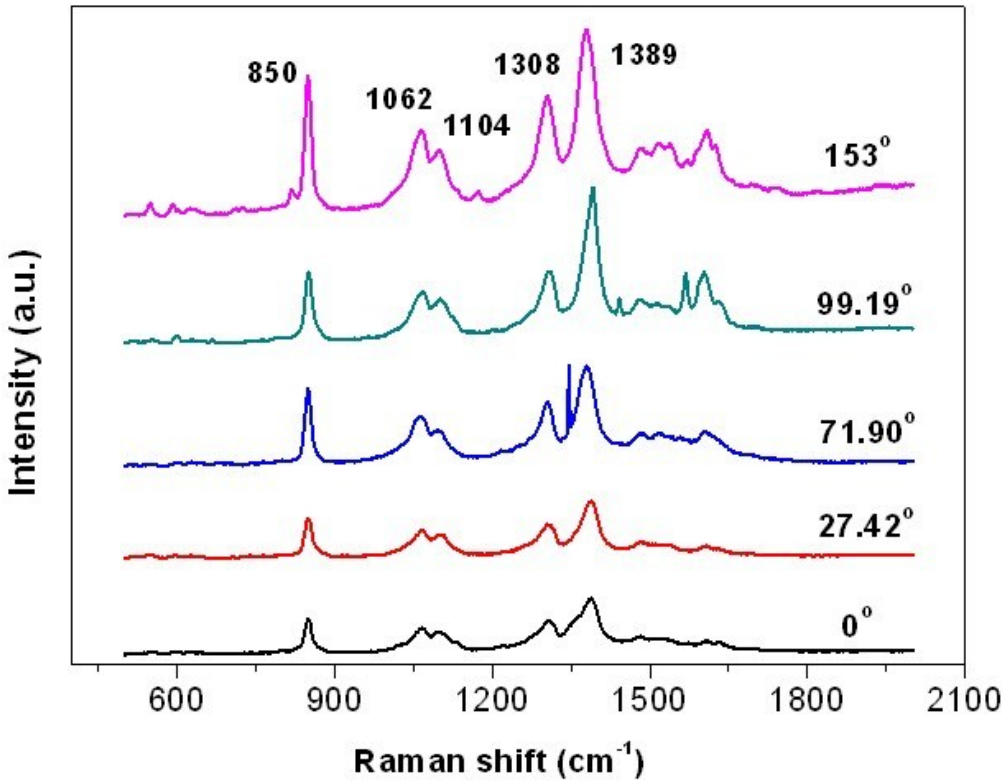

In addition, when the concentration of the explosives PA and NTO was 10^{-8} M, as the percentage of water in the mixed solvent increasing, SERS substrate and the water contact Angle increasing, also the hydrophobic property increasing, and the intensity of all the Raman peaks of PA and NTO increased gradually. Therefore, the stronger the hydrophobic effect of the solvent on the surface of the bionic AMA SERS substrate, the better the molecule could be concentrated into a small location, and the performance of the SERS sensor detection was better.

Table S3

Contact Angle (Water)		0°	27.42°	71.9°	111.8°	153°
Raman characteristic peaks' intensity of the explosive PA at 824 cm^{-1}	10^{-11}M	Failure	Failure	Failure	1044	1565
	10^{-8} M	3034	3092	3304	4664	5843
Raman characteristic peaks' intensity of the explosive NTO at 1389 cm^{-1}	10^{-11}M	1581	1645	3566	4017	4667
	10^{-8} M	6020	6689	11130	19287	20398

Figure S32 the possible effects of different storage style for SERS substrates on sensing detection NTO

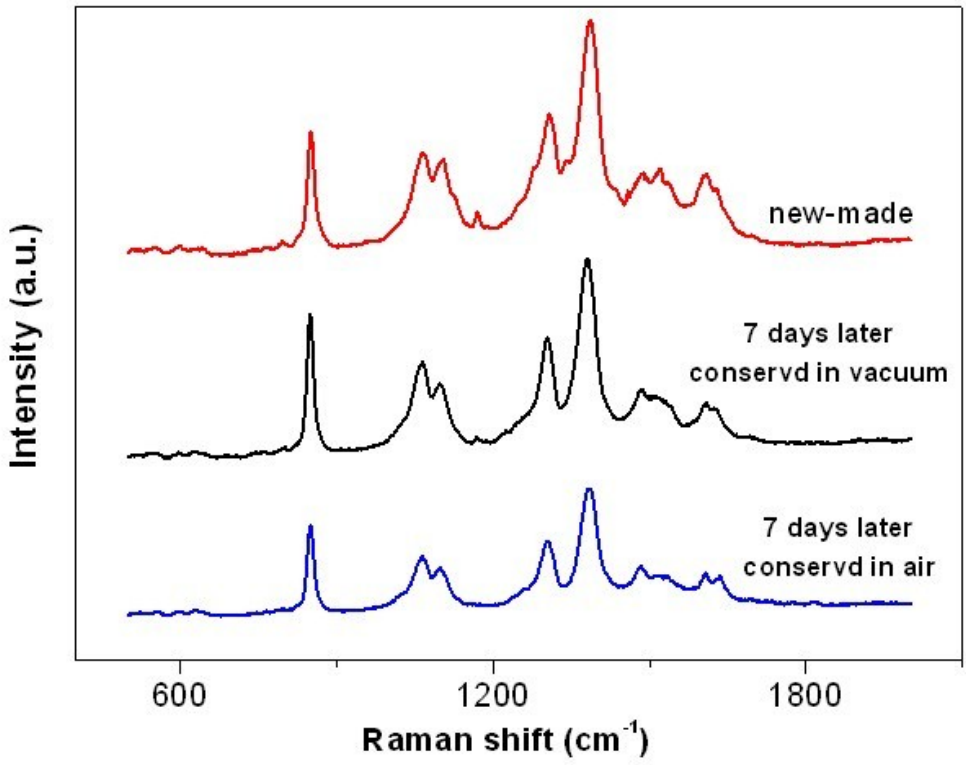

We divided the new prepared SERS substrates into two parts, one in the air and the other in a vacuum shading system. Seven days later, the SERS substrates were removed and detected the explosive NTO (10^{-10} M)

directly. Compared with the substrates placed in the vacuum shading system, the substrates placed in the air showed worse SERS enhanced performance. It was shown that when the substrates material was placed in the air, some silver nanosheets might be oxidized and the SERS activity was lost. But when the substrates were kept in a vacuum shielding system, the substrate activity could be maintained very well.

Reference

[1] Z. Huang, G. Meng, Q. Huang, Y. Yang, C. Zhu and C. Tang, *Adv. Mater.* **2010**, *22*, 4136.

[2] P. Srinivasan, M. Gunasekaran, T. Kanagasekaran, *Journal of Crystal Growth,* **2006**, *289*, 639.

[3] Xu, Z.; Meng, X. *Vibrational Spectroscopy*, **2012**, *63*, 390.